Satellite observations of formaldehyde over North America from GOME

Kelly Chance[1], Paul I. Palmer[2], Robert J.D. Spurr[1], Randall V. Martin[2], Thomas P. Kurosu[1], and Daniel J. Jacob[2]

Abstract. Formaldehyde (HCHO) is an important indicator of tropospheric hydrocarbon emissions and photochemical activity. We present HCHO observations over North America for July 1996 from the GOME instrument on-board the ESA ERS-2 satellite. Slant columns are determined to $<4\times10^{15}$ molecules cm^{-2} sensitivity by directly fitting GOME radiance measurements. These show a distinct enhancement over the southeastern United States, consistent with a large regional source from oxidation of non-methane hydrocarbons including in particular isoprene. Conversion of slant to vertical columns is done by combining species vertical distribution information from the GEOS-CHEM 3-D tropospheric chemistry and transport model with scattering weights from the Smithsonian Astrophysical Observatory LIDORT multiple scattering radiative transfer model. The results demonstrate the ability to measure HCHO from space in typical continental atmospheres, and imply that space-based measurements of HCHO may provide valuable information on emission fluxes of reactive hydrocarbons.

1. Introduction

Formaldehyde (HCHO) is a principal intermediate in the oxidation of hydrocarbons in the troposphere. Oxidation of methane (CH_4) by the hydroxyl radical (OH) is the principal source of HCHO in most of the troposphere; loss of HCHO is mainly by photolysis and reaction with OH. The corresponding atmospheric lifetime of HCHO is of the order of hours [*Logan et al.*, 1981]. Since CH_4 concentrations are relatively constant in the troposphere and photolysis is the dominant HCHO sink, when CH_4 is the dominant source a strong correlation is expected between HCHO concentrations and 24-hour average OH concentrations. Under these conditions, HCHO serves as a proxy for tropospheric OH [*Staffelbach et al.*, 1991].

In continental boundary layers, non-methane hydrocarbons (NMHCs) emitted by biogenic and anthropogenic sources usually dominate over CH_4 as a source of HCHO [*Munger et al.*, 1995; *Lee et al.*, 1998] and make a large contribution to the HCHO atmospheric column. There is considerable uncertainty regarding NMHC emission fluxes. National U.S. emission estimates of biogenic isoprene, an important precursor for ozone (O_3) smog, have increased by a factor of 5 over the past decade [*Guenther et al.*, 2000]. Emissions

of other biogenic NMHCs are even more uncertain. Inventories of NMHC emissions from automobiles are also difficult to constrain [*Pierson et al.*, 1990]. These uncertainties represent a major weakness in our ability to model ozone production [*McKeen et al.*, 1991], OH concentrations [*McKeen et al.*, 1997], formation of organic nitrates [*Moxim et al.*, 1996], and formation of organic aerosol [*Penner*, 1995]. Because HCHO is a major product of NMHC oxidation and its lifetime is short, it provides a diagnostic of integrated NMHC emissions and thus a test of emission inventories.

The Global Ozone Monitoring Experiment (GOME), launched on the ERS-2 satellite in April, 1995, obtains about 30,000 Earth radiance spectra each day. Spectra cover the ultraviolet ($237-405$ nm at 0.2 nm resolution) and the visible ($407-794$ nm at 0.4 nm resolution) [*Burrows et al.*, 1993; European Space Agency, 1995]. Current operational data products available for GOME include total columns of O_3 and NO_2, and cloud fractional coverage.

Preliminary HCHO measurement capability has been presented for GOME in *Thomas et al.* [1998]. We demonstrate here that it is now possible to determine HCHO columns from GOME spectra to sufficient precision (a factor of 4 to 5 improvement) for it to be used in detailed process studies as a tracer of NMHC emissions to the troposphere. The analysis method described here is applied to HCHO over North America in July 1996, where the source from oxidation of isoprene is expected to be particularly large over the southeastern U.S. [*Lee et al.*, 1998]. Under these conditions, most of the HCHO atmospheric column seen by GOME is in the continental boundary layer (this, and the details of the air-mass factor determination, are described in Palmer, P.I., D.J. Jacob, K. Chance, R.V. Martin, R.J.D. Spurr, T.P. Kurosu, I. Bey, R. Yantosca, A. Fiore, and Q. Li, Air-mass factor formulation for spectroscopic measurements from satellites: Application to formaldehyde retrievals from GOME, submitted to *J. Geophys. Res.,* 2000 - hereafter, PIP), so that the GOME measurements offer a proxy for emissions of NMHCs including in particular isoprene.

2. Spectrum Fitting

Vertical columns amounts of HCHO are determined in a two-step procedure. GOME radiance spectra are fitted first using a nonlinear least-squares inversion based on the Levenberg-Marquardt method [*Press et al.*, 1986]. The fitting process determines the slant column amounts that minimize the χ^2 error between observed and calculated GOME radiances. Second, a combination of radiative transfer calculations using the Smithsonian Astrophysical Observatory (SAO) LIDORT code [*Spurr et al.*, 2000] and results from the GEOS-CHEM global 3-D model of tropospheric chemistry and transport [*Bey et al.*, 1999] is used to determine the appropriate air-mass factors (AMFs) which convert the

[1]Harvard-Smithsonian Center for Astrophysics, Cambridge, MA

[2]Division of Applied Sciences, and Department of Earth and Planetary Sciences, Harvard University, Cambridge, MA
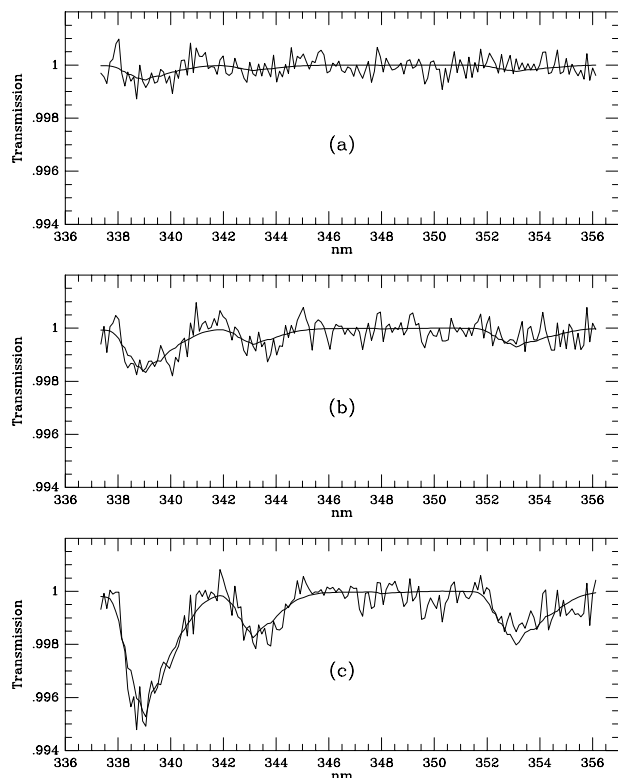
Figure 1. Fitting of HCHO in GOME orbit 70927023 for low, medium, and high HCHO amounts. (a) HCHO slant column $= 1.0\pm0.3 \times 10^{16}$ molecules cm^{-2}; (b) HCHO slant column $= 3.0\pm0.4 \times 10^{16}$ molecules cm^{-2}; (c) HCHO slant column $= 8.4\pm0.7 \times 10^{16}$ molecules cm^{-2}. Uncertainties from spectrum fitting and cross sections (including temperature dependence) are included. Absorptions for the fitted HCHO amounts are shown with and without the fitting residuals to allow vizualization of the fitting quality.

fitted slant columns to vertical column abundances. The GEOS-CHEM model uses assimilated meteorological data for July 1996. Vertical profiles of HCHO are sampled from that model for the time and location of each GOME observation. The AMF calculations are described in a separate paper (PIP).

HCHO slant columns are determined from GOME spectra by direct fitting of GOME radiances, as described in *Chance* [1998]. Individual radiance spectra are fitted, with no smoothing or filtering applied, over the wavelength region $337.35-356.12$ nm. This fitting window was determined as the optimum compromise between large intensity for the HCHO cross sections and small spectral interference; it is slightly different from that used in *Thomas et al.* [1998]. Reference spectra for HCHO, including linear temperature dependence, are from *Cantrell et al.* [1990]. The fitting includes the interfering species O_3, NO_2, BrO, and the O_2-O_2 collision complex. O_3 and BrO are fitted in separately optimized spectral windows, where their stronger absorption features are located, in order to determine their contributions in the HCHO fitting window as accurately as possible. The Ring effect is included as described in *Chance and Spurr* [1997]. Wavelength calibration of the GOME radiance and irradiance spectra in the level 1b operational data products is not sufficiently accurate to permit fitting to the required

levels. It is improved by using cross-correlation with the Fraunhofer reference spectrum [*Caspar and Chance*, 1997].

The GOME instrument suffers from substantial spectral undersampling. In regions where the atmospheric absorption is weak (e.g., that employed for HCHO fitting) this can largely be corrected using an undersampling correction spectrum generated by resampling an independent, high-resolution Fraunhofer reference spectrum [*Chance*, 1998; *Slijkhuis et al.*, 1999]. The resulting HCHO fits have residual rms values of typically 5×10^{-4} of the full-scale GOME radiance spectrum.

HCHO slant columns are determined to $<4.0\times 10^{15}$ molecules cm^{-2} fitting precision (1σ uncertainties are used throughout). Overall accuracies are determined by adding 5% uncertainty for the HCHO cross sections [*Cantrell et al.*, 1990] to the uncertainty from the fitting procedure, which is determined from the covariance matrix of the fitting errors and the rms of the fitting residuals. The fitting uses 300K cross sections. An additional 5% uncertainty is included to account for the temperature dependence of the cross sections; their integral changes by 5% over our spectral fitting range in going from 300K to 270K. This temperature range is appropriate for the HCHO observations presented here, considering that the bulk of the HCHO column is in the lower troposphere (PIP). Figure 1 shows spectral fitting examples
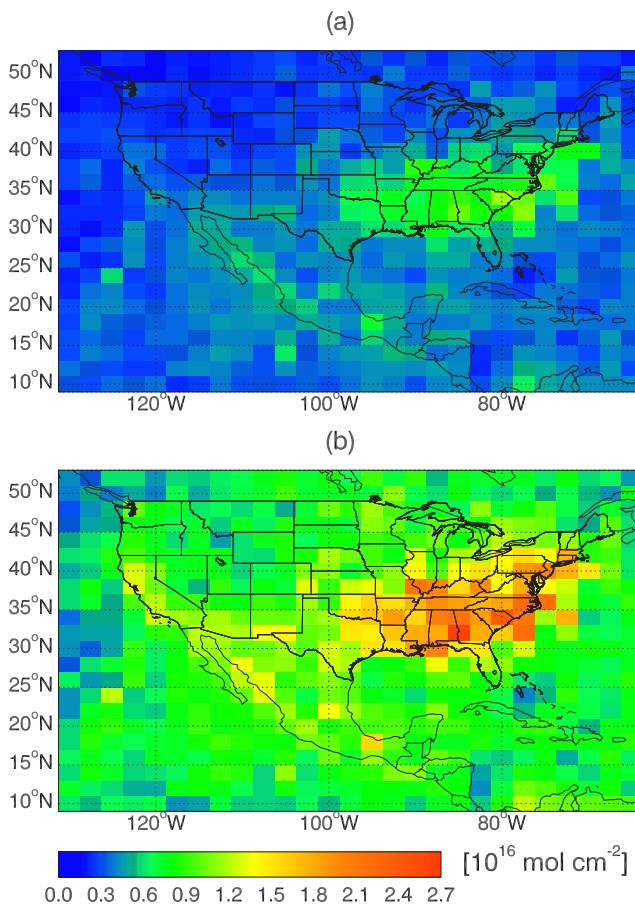
Figure 2. HCHO columns retrieved from the GOME instrument over the U.S. for July 1996. Observations are for 1026-1154 local solar time and for cloud cover less than 40%. Figure 2a shows the geometric total vertical columns and Figure 2b show the total vertical columns which account for Rayleigh scattering.

for low, moderate, and high concentrations of HCHO, plotted as the fitted absorption of HCHO with and without the fitting residuals.

3. Results

HCHO columns have been retrieved for $0°-75°$N, $45°-180°$W for the entire month of July 1996. Results for the North American region, $10°-60°$N, $65°-130°$W, selected for cloud fractional coverage of less than 40% and binned on a $2°×2.5°$ grid, are shown in Figure 2a, after division by geometric air-mass factors AMF_G, where $AMF_G = \sec\theta_s + \sec\theta_v$, θ_s is the solar zenith angle, and θ_v the satellite viewing zenith angle. The solar zenith angles and solar times corresponding to these measurements range from $15-35°$ and $1026-1154$, respectively; the range of satellite viewing angles is $0°-31°$. The resulting AMF_G values range from 2.0 to 2.4.

Figure 2b shows the vertical columns of HCHO obtained after determination of AMFs that account for Rayleigh scattering, as described above. These AMFs are in the range $0.7-1.2$, about half of the geometric AMFs because most of the HCHO is in the lower troposphere where scattering inhibits viewing. Variability in the shape of the vertical profile of HCHO in the GEOS-CHEM model induces $\sim$20% variability in the AMFs. We find a large HCHO enhancement over southeastern United States, as expected from the strong regional source contributed by oxidation of isoprene [*Lee et al.*, 1998]. This enhancement is manifest from the spectral analysis alone (Figure 2a) and is magnified by application of the scattering AMF (Figure 2b). This reflects the a priori information from the GEOS-CHEM model that most of the HCHO column is in the boundary layer (PIP). The HCHO columns over the southeastern U.S. in Figure 2b are in the range $2-3×10^{16}$ molecules cm^{-2}. Assuming a typical HCHO scale height of 2 km [*Lee et al.*, 1998], these columns correspond to boundary layer concentrations of $4-6$ ppbv, which are consistent with in situ observations in that region [*Munger et al.*, 1995; *Lee et al.*, 1998].

In the future, this work will be expanded to include detailed studies of HCHO emissions over the U.S. in other years and seasons, and in greater temporal detail, to test estimates of isoprene emission fluxes and identify hot spots. The July 1996 data shown here contain much more detail about local production and transport than is provided in the present overview. We will also extend our analysis to the tropics, where biogenic and biomass burning sources of NMHCs are highly uncertain.

Future work should include improvement in the retrieval of HCHO. With improved HCHO sensitivity, or by merging results over selected regions, we will investigate HCHO in the remote marine troposphere. Better quantification of HCHO requires improvements in cloud and aerosol determination. Clouds mask the HCHO from observation. Scattering by aerosols alters the effective path length for HCHO absorption, enhancing or decreasing the observed HCHO absorption, depending on the measurement geometry, the vertical distribution of the aerosol relative to that of HCHO, and the surface albedo. For severe haze events, with scattering aerosol optical depths at 340 nm (τ_{340}) of the order of 2 in the boundary layer, the AMF may increase by 40% (PIP). Improved cloud parameterization will come from the Cloud Retrieval Algorithm for GOME (CRAG) [*Kurosu et*

al., 1999], which has been developed to provide cloud fractional coverage, cloud-top height, and optical thickness for the GOME scenes.

References

Bey, I., D.J. Jacob, R.M. Yantosca, J.A. Logan, B.D. Field, A.M. Fiore, Q. Li, H. Liu, and M.G. Schultz, Asian outflow to the Pacific Ocean in springtime: A 3D simulation of the PEM-West (B) mission with assimilated meteorology, submitted to *J. Geophys. Res.*, August 2000.

Burrows, J.P., K.V. Chance, A.P.H. Goede, R. Guzzi, B.J. Kerridge, C. Muller, D. Perner, U. Platt, J.-P. Pommereau, W. Schneider, R.J. Spurr, and H. van der Woerd, *Global Ozone Monitoring Experiment Interim Science Report*, ed. T. D. Guyenne and C. Readings, Report ESA SP-1151, ESA Publications Division, ESTEC, Noordwijk, The Netherlands, ISBN 92-9092-041-6, 1993.

Cantrell, C.A., J.A. Davidson, A.H. McDaniel, R.E. Shetter, and J.G. Calvert, Temperature-dependent formaldehyde cross sections in the near-ultraviolet spectral region, *J. Phys. Chem. 94*, 3902-3908, 1990.

Caspar, C., and K. Chance, GOME wavelength calibration using solar and atmospheric spectra, *Proc. Third ERS Symposium on Space at the Service of our Environment,* Ed. T.-D. Guyenne and D. Danesy, European Space Agency publication SP-414, ISBN 92-9092-656-2, 1997.

Chance, K., and R.J.D. Spurr, Ring effect studies: Rayleigh scattering, including molecular parameters for rotational Raman scattering, and the Fraunhofer spectrum, *Appl. Opt. 36*, 5224-5230, 1997.

Chance, K., Analysis of BrO measurements from the Global Ozone Monitoring Experiment, *Geophys. Res. Lett. 25*, 3335-3338, 1998.

European Space Agency, *The GOME Users Manual,* ed. F. Bednarz, European Space Agency Publication SP-1182, ESA Publications Division, ESTEC, Noordwijk, The Netherlands, ISBN-92-9092-327-x, 1995.

Guenther, A., C. Geron, T. Pierce, B. Lamb, P. Hatley, and R. Fall, Natural emissions of non-methane volatile organic compounds, carbon monoxide, and oxides of nitrogen from North America, *Atmos. Env. 34*, 2205-2230, 2000.

Horowitz, L.W., J. Liang, G.M. Gardner, and D.J. Jacob, Export of reactive nitrogen from North America during summertime: Sensitivity to hydrocarbon chemistry, *J. Geophys. Res. 103,* 13,451-13,476, 1998.

Kurosu, T.P., K.V. Chance and R.J.D. Spurr, CRAG – Cloud Retrieval Algorithm for ESA's Global Ozone Monitoring Experiment, *Proc. 1999 European Symposium on Atmospheric Measurements from Space,* ESA WPP-161, 513-521, 1999.

Lee Y.-N., et al., Atmospheric chemistry and distribution of formaldehyde and several multioxygenated carbonyl compounds during the 1995 Nashville/Middle Tennessee Ozone Study, *J. Geophys. Res. 103*, 22,449-22,462, 1998.

Logan, J.A., M.J. Prather, S.C. Wofsy, and M.B. McElroy, Tropospheric chemistry: A global perspective, *J. Geophys. Res. 86,* 7210-7254, 1981.

McKeen, S.A., E.-Y. Hsie, and S.C. Liu, A study of the dependence of rural ozone on ozone precursors in the Eastern United States, *J. Geophys. Res. 96,* 15,377-15,394, 1991.

McKeen, S.A., *et al.*, Photochemical modeling of hydroxyl and

its relationship to other species during the Tropospheric OH Photochemistry Experiment, *J. Geophys. Res. 102,* 6467-6493, 1997.

Moxim, W.J., H. Levy II, and P.S. Kasibhatla, Simulated global tropospheric PAN: Its transport and impact on NO_x, *J. Geophys. Res. 101,* 12,621-12,638, 1996.

Munger, J.W., D.J. Jacob, B.C. Daube, L.W. Horowitz, W.C. Keene, and B.G. Heikes, Formaldehyde, glyoxal, and methylglyoxal at a rural mountain site in central Virginia, *J. Geophys. Res. 100,* 9325-9334, 1995.

Penner, J.E., Carbonaceous aerosols influencing atmospheric radiation: Black and organic carbon, in *Aerosol Forcing of Climate*, edited by R.J. Charlson and J. Heintzenberg, pp. 91-108, J. Wiley & Sons, 1995.

Pierson, W.R., A.W. Gertler, and R.L. Bradow, Comparison of the SCAQS tunnel study with other on-road vehicle emission data, *J. Air Waste Manage. Assoc. 40,* 1495-1504, 1990.

Press, W.H., B.P. Flannery, S.A. Teukolsky, and W.T. Vetterling, *Numerical Recipes,* ISBN 0-521-30811-9, Cambridge University Press, 1986.

Slijkhuis, S., A. von Bargen, W. Thomas, and K. Chance, Calculation of undersampling correction spectra for DOAS spectral fitting, Proc. ESAMS'99 - European Symposium on Atmospheric Measurements from Space, ESA WPP-161, ISSN 1022-6656, 563-569, 1999.

Spurr, R.J.D., T.P. Kurosu and K.V. Chance A linearized discrete ordinate radiative transfer model for atmospheric remote sensing retrieval, *J. Quant. Spectrosc. Rad. Transfer*, in press, 2000.

Staffelbach, T., A. Neftel, B. Stauffer, and D.J. Jacob, Formaldehyde in polar ice cores: A possibility to characterize the atmospheric sink of methane in the past?, *Nature 349*, 603-605, 1991.

Thomas, W., E. Hegels, S. Slijkhuis, R. Spurr, and K. Chance, Detection of biomass burning combustion products in Southeast Asia from backscatter data taken by the GOME spectrometer, *Geophys. Res. Lett. 25*, 1317-1320, 1998.

K. Chance, T.P. Kurosu, and R.J.D. Spurr, 60 Garden Street, Cambridge, MA 02138
(email: kchance; tkurosu; rspurr@cfa.harvard.edu)

D.J. Jacob, R.V. Martin, and P.I. Palmer, 29 Oxford Street, Cambridge, MA 02138
(email: djj; rvm; pip@io.harvard.edu)